JOURNAL OF APPLIED ELECTROCHEMISTRY 24 (1994) 1249–1255

Properties of Zn–Ni alloy deposits from ammonium baths*

G. BARCELÓ, J. GARCÍA, M. SARRET, C. MÜLLER‡

Departament de Química Física, Universitat de Barcelona, Martí i Franquès 1, 08028 Barcelona, Spain

J. PREGONAS

PREMA S.A. Company. Benages s/n, Capellades, Spain

Received 30 November 1993; revised 30 March 1994

Zinc–nickel alloys have been electrodeposited from a simple bath containing only zinc, nickel and ammonium chlorides. The composition, morphology, structure and corrosion resistance of the alloys obtained with this bath have been studied and the influence of some additives, normally used to reduce the stress of the deposits, has also been analysed. Among these additives it has been found that the aromatic sulfonimide does not significantly modify the deposit characteristics but improves the corrosion resistance of the alloys. Moreover, the applicability of two statistical methods to a deposition process has been tested, to obtain the main factor determining the deposit composition.

1. Introduction

Zinc alloy deposition has been of interest recently since such alloys provide better corrosion protection than unalloyed zinc coatings. Zinc–nickel alloys have received more attention than other zinc alloy deposits because of their high degree of corrosion resistance and their mechanical properties. Various electrolytes have been reported for depositing Zn–Ni of different composition [1–7]. In previous studies by this group, Zn–Ni electroplates were obtained from a complex bath containing two or three organic additives, which led to alloys with a low percentage of nickel but good corrosion resistance [8–10].

At present, galvanic industries usually use ammonium baths to obtain zinc–nickel alloys with a nickel content between 10–15%, since it seems that this composition provides the best corrosion protection [11, 12]. Fratesi and Roventi studied the influence of different parameters, essentially on the transition current, and also on phase and morphology of the alloys obtained from a bath containing high concentrations of ammonium chloride and boric acid [7]. In the present study, Zn–Ni electroplates were also obtained from an ammonium bath under industrial conditions, in order to analyse the characteristics of the deposits obtained using different plating conditions. The electrolyte used in this case contained zinc, nickel and ammonium chlorides and also additives, selected from those usually used to reduce the stress in metallic deposition. This new bath was selected because its composition is simple and all the components can be obtained with a high degree of purity. Therefore, future studies of the deposition process can be carried out in controlled conditions (pure chemicals and electrodes) and may provide further information. Results may then be compared with those obtained under the industrial conditions used in the present study.

Moreover, since this ammonium electrolyte is simpler than others developed previously at this laboratory, it has been selected to test the applicability of two different statistical methods to a deposition process: a four-level orthogonal design to determine the first-order influence of each factor on the response [13] and a two-level factorial design to estimate the interactions between the different parameters [14].

2. Experimental details

Zinc–nickel electrodeposits were obtained under galvanostatic conditions, to a constant thickness of 10 μm. The baths contained $ZnCl_2$ (20–65 g dm^{-3} Zn^{2+}), $NiCl_2 \cdot 6H_2O$ (2–23 g dm^{-3} Ni^{2+}) and NH_4Cl (150–260 g dm^{-3}); pH was between 4.8 and 5.8 and was obtained by adding HCl or NH_3. All solutions were prepared using deionised water and reagent grade chemicals. In some experiments organic compounds were added to the bath (an aromatic sulfonimide, A1, an acetylene alcohol, A2, and a chlorohydrated imine, A3) in amounts between 1.0 g dm^{-3} and 5.0 g dm^{-3}.

Except when the influence of temperature was studied, the alloys were usually obtained at 25 °C. During the electrodeposition process the cathode potentials were measured using a Ag/AgCl electrode.

A methacrylate cell with a capacity of 1.5 dm^{-3} was used and the alloys were obtained on both sides of iron plates (exposed area 16 cm^2). The anodes were

* Presented in part at the 44th meeting of ISE, Berlin, September 1993.
‡ To whom correspondence should be addressed.

0021-891X

Table 1. Influence of temperature and NH_4Cl concentration on the $\%Ni_{dep}$ for a bath containing 35 g dm^{-3} of Zn^{2+} and 12 g dm^{-3} of Ni^{2+} at pH 5.6 and 3.13 A dm^{-2}

$[NH_4^+]$	T	Ni_{dep}
g dm^{-3}	°C	/%
220	25	11.8
220	35	13.1
220	42	14.0
150	25	9.4
260	25	12.4

of zinc, with an exposed area of 90 cm^2. Before deposition, the cathode was polished with emery paper, washed electrochemically in a strong basic solution and neutralised in 10% HCl solution. After deposition, the deposits were washed with deionised water and dried in warm air.

To analyse the corrosion resistance of the alloys, some deposits were chromated by immersion for 25–60 s at 25 °C in a chromating solution containing 15 g dm^{-3} Cr^{6+} at pH 1.8 (HCl). After this process the deposits were rinsed in deionised water, dried in warm air and subjected to the salt-spray test, after ageing at room temperature for at least 24 h.

The composition of the alloys was determined by means of absorption spectrophotometry and their morphology was observed by optical microscopy (OM) and by scanning electron microscopy (SEM). The deposit phases were analyzed by X-ray diffraction and the composition profiles were studied by ESCA.

3. Results

3.1. *Effect of operating variables on alloy composition*

The first step in the optimization of a process is to determine which factors and which interactions are important in affecting the response. This process can be carried out using factorial design.

In the present case, at a given current density, the influence of five parameters on the composition of the alloys was analysed: the concentrations of zinc, nickel and ammonium chloride, the pH and the temperature. To reduce the number of variables, the first step in this study was to analyse the influence of temperature on the $\%Ni_{dep}$ and then, to select the most economical conditions that lead to good deposits. As expected, an increase in the plating temperature caused an increase in the nickel content of the alloys (Table 1). For most electrolytes analysed the % Ni_{dep} obtained at 25 °C was between 10–14% over a wide interval of current densities and, since these values were in the range of which Zn–Ni electroplates show the best anticorrosion behaviour, this temperature was selected to analyse the effect of the other factors on the composition of the deposits.

The percentage of nickel deposited increased slightly with the ammonium concentration (Table 1),

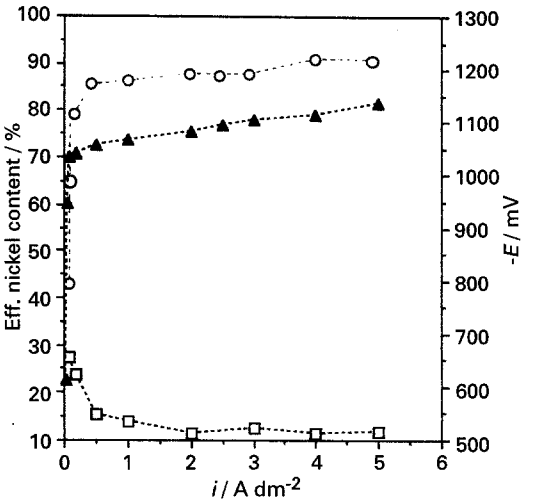

Fig. 1. Effect of current density on nickel content of deposits (□), on current efficiency for alloy deposition (○) and polarization curve (▲) during the deposition process. $[Zn^{2+}] = 35$ g dm^{-3}, $[Ni^{2+}] = 12$ g dm^{-3}, pH 5.6.

but with the highest amounts there were solubility problems at low temperatures and, therefore, a value of 220 g dm^{-3} was selected in most cases. With temperature and NH_4Cl concentration fixed at these values, at a given current density, three factors were considered to determine the $\%Ni_{dep}$: the concentrations of Zn and Ni in the bath and the pH.

To test the applicability of the four-level orthogonal design, four levels of Ni^{2+} concentration were selected between 12 g dm^{-3} and 23 g dm^{-3} and for Zn^{2+} four concentrations were selected between 35 g dm^{-3} and 60 g dm^{-3}. The pH was set to four values between 5.0 and 5.8. For the two-level factorial design only the lowest and highest values were considered for each parameter. It was found that the main factor determining the composition of the alloys was the concentration of Ni^{2+} followed by the pH and, finally, the Zn^{2+} concentration. Moreover, within the intervals considered, the factorial design did not predict any interaction between these parameters. The best deposits were obtained from electrolytes containing from 12 to 17 g dm^{-3} of Ni^{2+}, from 30 to 45 g dm^{-3} of Zn^{2+} and at pH between 5.5 and 5.7. These alloys had a nickel content between 12–14% (at 2.0 A dm^{-2}), were uniform and compact and the current efficiency of the deposition process was about 90%. Different experiments carried out classically lead to the same conclusions and, therefore, it seems that a statistical method could be applied in other cases to a more complex electrolyte to evaluate the influence of the different factors on the alloy composition and to optimize the deposition conditions.

Figure 1 shows the effect of current density on the alloy composition and current efficiency, together with the polarization curve for these optimized baths. As observed in other cases [7, 8], the percentage of nickel was approximately constant over a wide range of current densities and increased strongly at the lowest current densities. This increase in the % Ni_{dep} coincided with a sharp decrease in potential and current efficiency.

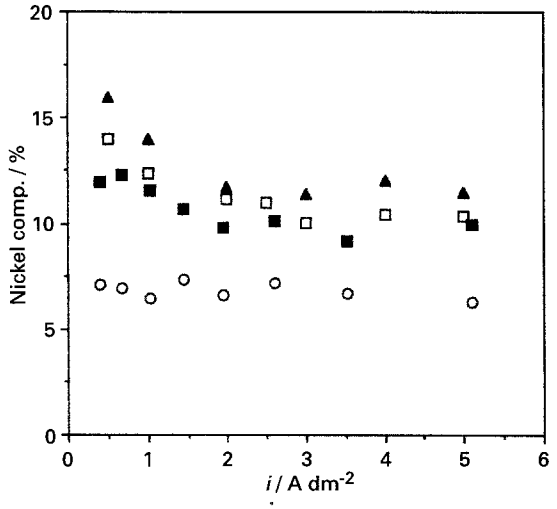

Fig. 2. Composition of the alloys obtained at different current densities from a bath without additives (□) or containing 2.0 g dm^{-3} of A1 (▲), A2 (■) and A2 + A3 (○). [Zn^{2+}] = 41 g dm^{-3}, [Ni^{2+}] = 15 g dm^{-3} pH 5.6.

Various organic compounds were added to the bath to improve the appearance of the deposits and reduce stress. The concentration of additives was varied between 1.0 g dm^{-3} and 5.0 g dm^{-3} and the appearance and composition of the alloys was the same within the interval 2.0–5.0 g dm^{-3}. Figure 2 shows the comparison between the percentage of nickel obtained from a bath without additives and those obtained with added compounds. Additive A1 caused a slight increase in the nickel content, while with A2 the %Ni_{dep} was unmodified or was slightly lower; with the imine A3 or in combination with other additives the percentage of nickel deposited always decreased markedly.

The effect of these additives on the deposition potential was, in all cases, to shift the potential to more positive values (Table 2), while none of them markedly affected the efficiency of the deposition process.

3.2. *Morphology and microstructure of the deposits*

With this ammonium electrolyte homogeneous and bright or semibright deposits were obtained with current density up to 7.0 A dm^{-2}. The surface morphology of the alloys was examined by scanning electron microscopy (SEM). Figures 3 and 4 show the

Table 2. Deposition potentials obtained with an additive-free bath, [Zn^{2+}] = 41 g dm^{-3}, [Ni^{2+}] = 15 g dm^{-3}, pH 5.6, or containing 4.0 g dm^{-3} of the different additives

	−E/mV vs Ag/AgCl				
i/A dm^{-2}	free	A1	A2	A3	A2 + A3
5.0	1159	1090	1078	1083	1086
4.0	1130	1080	1075	1078	1076
3.0	1104	1075	1070	1073	1074
2.0	1080	1062	1058	1065	1070
1.0	1066	1052	1050	1053	1056
0.5	1057	1046	1040	1040	1050

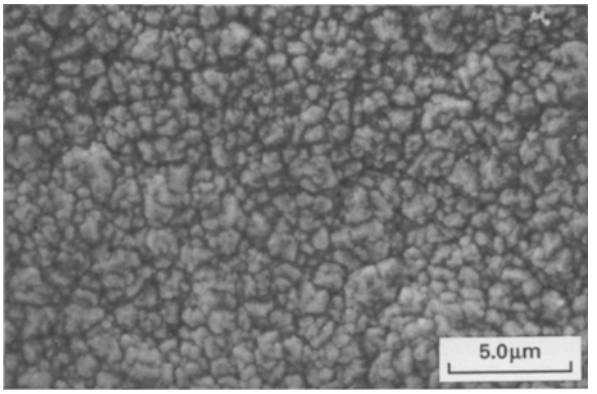

Fig. 3. Microstructure of a Zn–Ni alloy obtained without additives and containing 11.2% nickel. Current density 2.0 A dm^{-2}.

structural details of some zinc-nickel deposits obtained from the pure-electrolyte. It was observed that the deposit morphology depended on the alloy nickel content and also on the current density: between 10% and 12% nickel (Fig. 3) the deposits obtained at high current densities had a quasi nodular appearance, while those obtained at low current densities presented larger grains with sharp edges. When the percentage of nickel increased (Fig. 4), pyramidal crystallites, with a more regular distribution at low current densities, were observed.

For deposits produced in baths containing additives, the SEM pictures showed that the deposits were more compact, but the grain sizes were not reduced significantly (Figs 5–7). The boric electrolyte studied previously contained three different additives and each one promoted a shift of deposition potential to more negative values [9]; these additives were adsorbed on the cathode surface, the deposition process was hindered and a more negative potential was required in order to reach a given rate of deposition. This decrease in the potential resulted in an increase in nucleation over growth and the deposits were more compact with a finer grain size. In the present case, the additives tested with the ammonium bath were not typical brighteners, the potential measured in the additive-containing bath was always slightly more positive than that obtained without additives (Table 2) and, therefore, the grain sizes were not reduced.

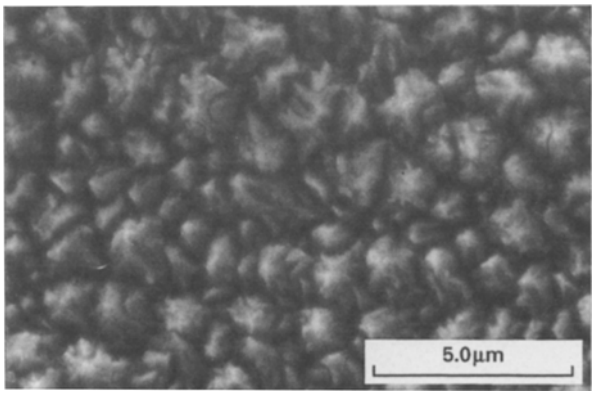

Fig. 4. Microstructure of a Zn–Ni alloy obtained without additives and containing 16.7% nickel. Current density 2.0 A dm^{-2}.

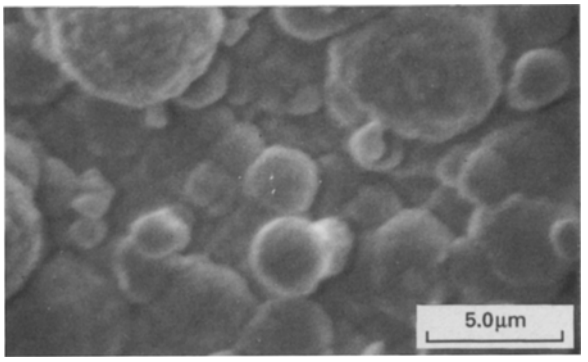

Fig. 5. SEM picture of a Zn–Ni alloy 9.3% nickel obtained with additive A3 at 2.0 A dm^{-2}.

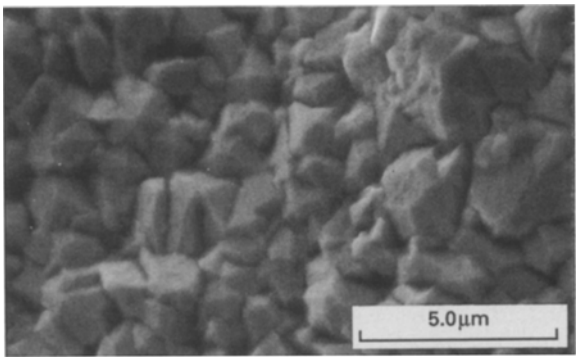

Fig. 6. SEM picture of a Zn–Ni alloy 12.6% nickel obtained with additive A1 at 2.0 A dm^{-2}.

On the other hand, there was a clear influence of the different additives on the grain shape. The deposits obtained with A3 or in combination with other compounds always presented a nodular appearance and were irregular with emerging grain agglomerations (Fig. 5). With A1 (Fig. 6) or A2 (Fig. 7), regardless of current density used, a homogeneous structure formed by pyramidal crystallites was observed.

The surface structures of chromate films formed upon Zn–Ni coatings displayed no substantial differences, regardless of immersion time used (25–60 s). The SEM photographs showed a very uniform surface with the pyramidal crystallites rounded, but without the cracks observed in other deposits of this kind [15, 16].

The phases of the deposits were identified by diffractometric analysis. Figure 8 shows the X-ray diffractograms obtained for alloys of different composition from 7.0% to 24.0% nickel. The composition range of the pure γ phase was between 10% and 25% nickel for the Zn–Ni coatings obtained from the pure-electrolyte. Alloys with lower nickel content were dual-phase, $\gamma + Zn$. The δ phase was not discernible from the XRD data.

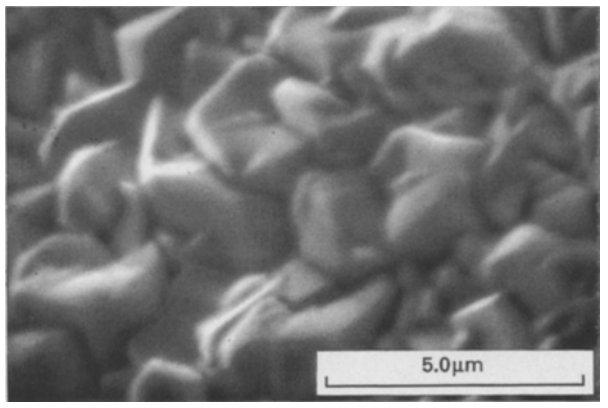

Fig. 7. SEM picture of a Zn–Ni alloy 13.1% nickel obtained with additive A2 at 0.5 A dm^{-2}.

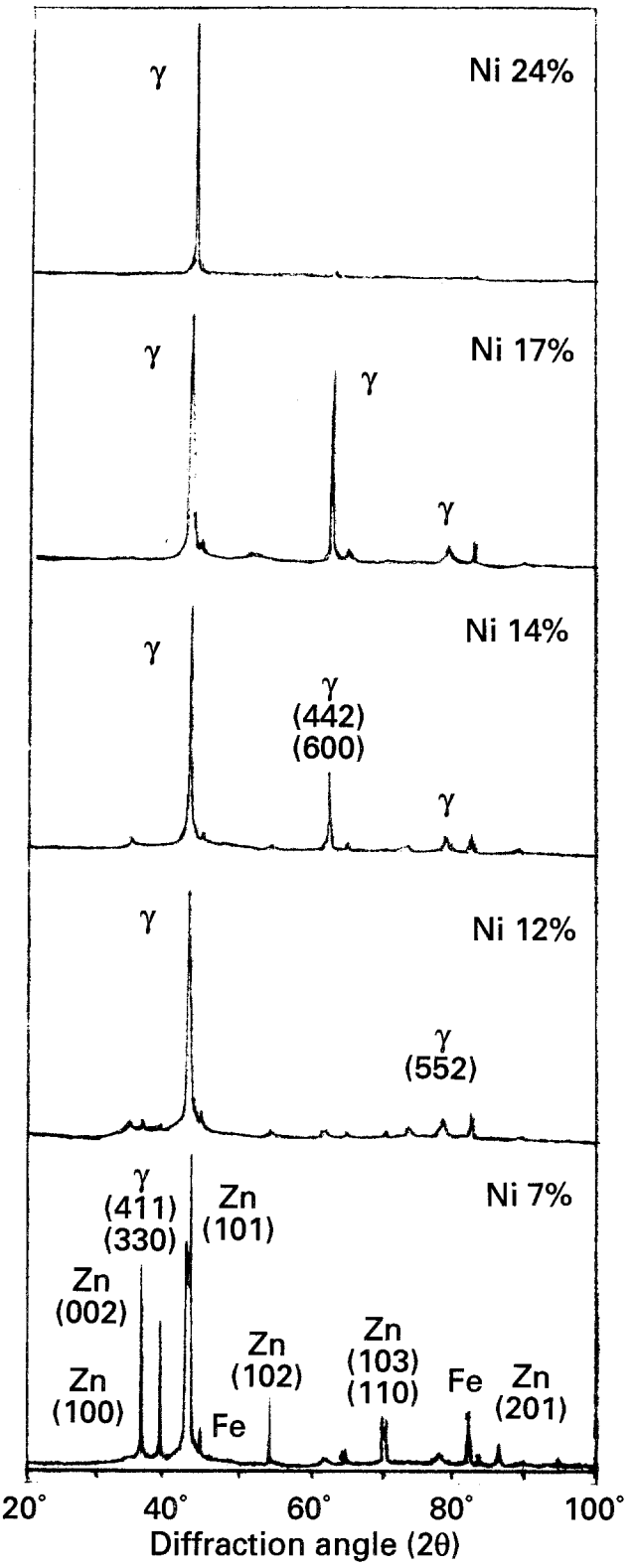

Fig. 8. X-ray diffraction profiles of different alloy composition obtained at 2.0 A dm^{-2} from a bath without additives. $[Zn^{2+}] = 35\ g\,dm^{-3}$ and different Ni^{2+} concentrations.

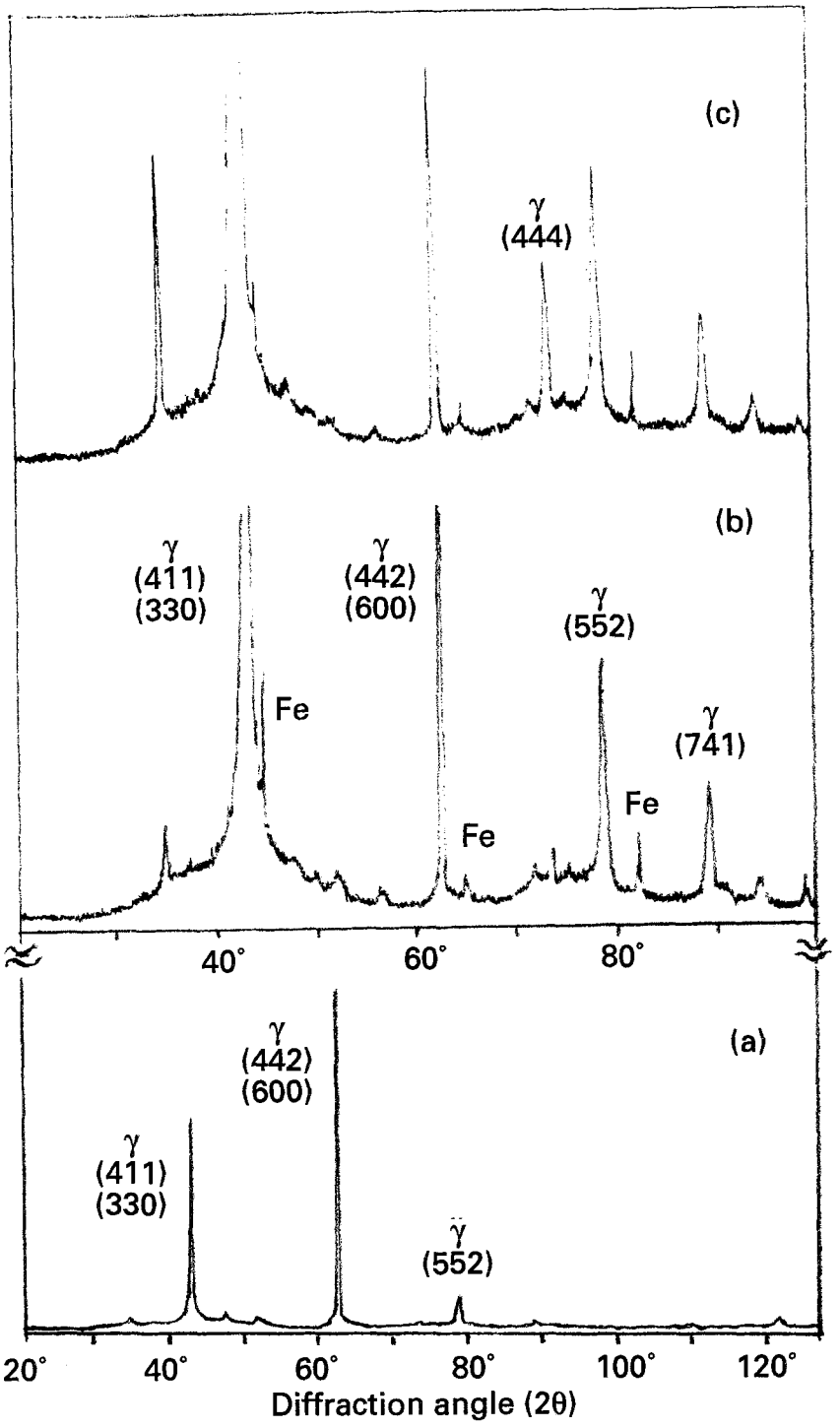

Fig. 9. X-ray diffraction profiles of Zn–Ni alloys obtained from a bath containing $[Zn^{2+}] = 41\,g\,dm^{-3}$, $[Ni^{2+}] = 15\,g\,dm^{-3}$. (a) [A1] = 0.0 g dm^{-3}, 0.25 A dm^{-2}, $\%Ni_{dep} = 24.2$; (b) [A1] = 0.0g dm^{-3}, 2.0 A dm^{-2}, $\%Ni_{dep} = 11.8$; (c) [A1] = 2.0 g dm^{-3}, 2.0 A dm^{-2}, $\%Ni_{dep} = 12.1$.

The highest reflection intensity of the γ phase usually corresponded to the (3 3 0) and (4 1 1) preferential orientations, although (4 4 2) and (6 0 0) orientations were also observed at nickel contents over 10%. Figure 9(a) and (b) show the diffractograms of 24% and 12% nickel alloys obtained with different baths or with different current density from the alloys shown in Fig. 8. By comparing the Figures it is observed that the preferential orientation of γ phase depends not only on the deposit composition, but also on the bath composition and plating conditions.

The deposits obtained from additive-bearing baths presented similar characteristics: when A1 or A2 were used the γ phase was observed, with a small presence of zinc phase below 10% nickel, while the alloys obtained with A3 or in combination with other additives always showed the two-phase structure (γ and Zn) with only the (3 3 0) preferential orientation.

Although the diffractograms obtained in the presence and absence of additives were similar, the imide A1 always promoted an intensity increase of a peak at 34.1° (Fig. 9(c)) which, according to the PDF tables, does not correspond either to Zn or to any Zn–Ni phase. This peak has been observed in other cases [17] in a 30% Ni alloy and has been assigned to the (3 2 1) preferred orientation of a complex cubic γ' phase, while, with the lattice parameter of the cubic γ phase ($a = 0.892$ nm), this peak should correspond to the crystallographic plane (2 2 2). Taking into

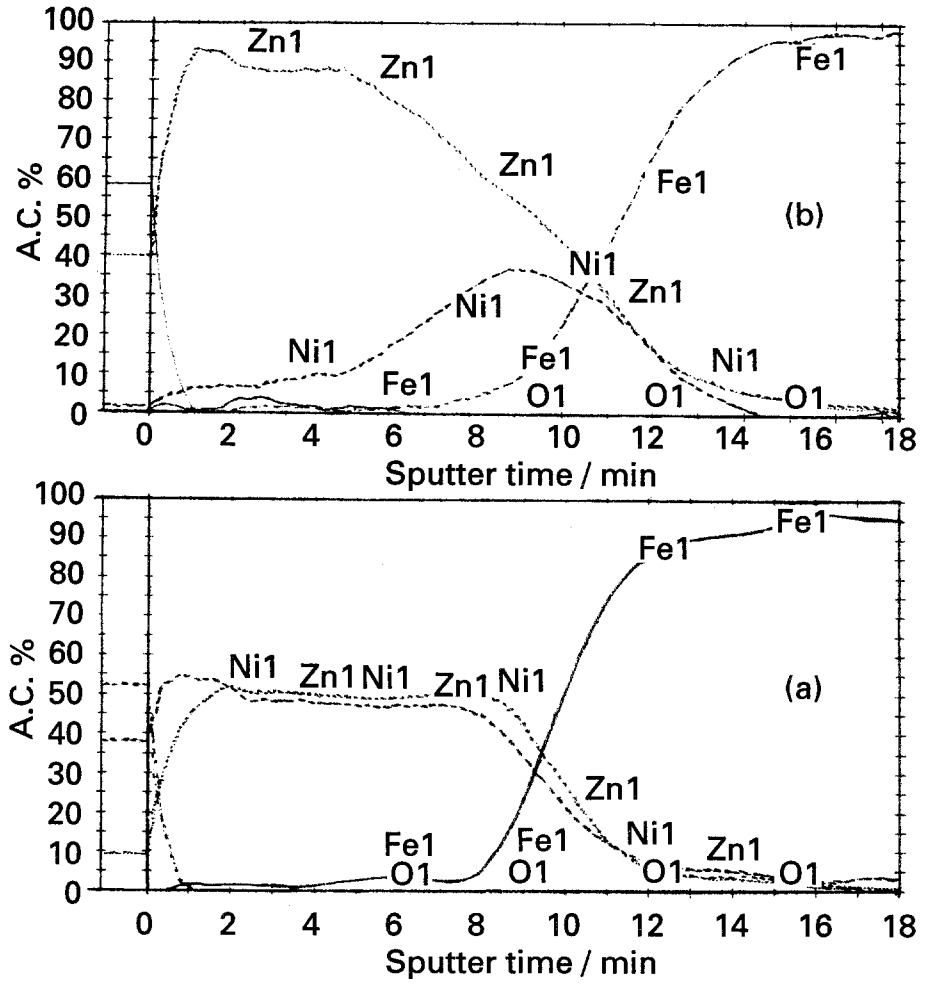

Fig. 10. ESCA depth profiles of Zn–Ni alloys containing (a) 14.1% nickel and (b) 6.8% nickel.

account that when this peak increased, so did the peak corresponding to the (4 4 4) orientation, and that the position of all other peaks corresponded to the normal γ phase, this peak may correspond to the (2 2 2) preferred orientation of the γ phase.

Finally, the composition profile along the depth of the deposits was studied by ESCA analysis. The profiles obtained for different alloy composition always showed three zones (Fig. 10): the surface oxides, corresponding essentially to zinc oxides, the Zn–Ni deposit which was fairly uniform in composition, and a zone of intermetallic diffusion. The profiles presented evidence of preferential sputtering of zinc, since the percentage of zinc in the deposits was always lower than that determined by absorption spectrophotometry. This has been observed in other cases when the alloy constituents differ appreciably in their heats of sublimation, and the energy of sublimation of zinc is lower than that of nickel by a factor of three [18]. This preferential sputtering of zinc was less important for the alloys containing low nickel percentages, obtained with or without additives, which also presented less uniform composition profiles, with a higher nickel content on the first deposit layers (Fig 10(b)). This deposition process is now being analysed under controlled conditions (pure chemicals and electrodes) and electrochemical analysis shows that this is not a sputtering effect: the stripping of alloys obtained at the same potential, but with different deposition times, shows that the percentage of nickel really decreases with deposition time. On the other hand, the first composition profiles of zinc–nickel alloys of similar composition, but obtained from a different bath now being developed in our laboratory, do not present this phenomenon of preferential sputtering of zinc and so the alloy composition determined by ESCA coincides with that obtained by absorption spectrophotometry. Therefore, the preferential sputtering of zinc is not merely a consequence of the difference between the sublimation heats of zinc and nickel, and other factors, such as composition or structure, should be considered.

3.3. *Corrosion resistance*

The corrosion resistance of the alloys was evaluated by observing the propagation of red rust formed on the deposits, tested in a 5% neutral salt-spray environment at 35 °C. For the passivated alloys, the propagation of white rust was also observed.

When the additive A2 was used, the corrosion resistance of the alloys was very similar to that obtained with the free-additive bath (Table 3), it was improved with A1 and clearly worsened with A3 or with its combinations. The corrosion resistance of the chromated alloys was excellent. For example, white rust did not appear for more than 1300 h and red rust for more than 2700 h on the first deposit shown in Table 3.

Table 3. Hours until the appearance of 1% of red rust for alloys obtained at 2.0 A dm^{-2} from baths without additives ([Zn^{2+}] = 41 g dm^{-3}, [Ni^{2+}] = 15 g dm^{-3}, pH 5.6) or containing 2.0 g dm^{-3} of the different additives

Additive	Ni_{dep} /%	*Time to red rust appearance* /h
–	10.9	1248
A1	11.8	1344
A2	9.5	1272
A3	6.8	744

The corrosion resistance of the alloys obtained with A3 was always lower than that observed in other cases because the nickel content of these alloys was also lower (Fig. 2), but the corrosion behaviour of the alloys was even worse than that observed previously for alloys containing 1–2% of nickel, obtained from a boric bath [9, 10]. This unsatisfactory corrosion behaviour could be due to the dual-phase $\gamma + Zn$, which is known to be less resistant to salt corrosion than pure γ [1], and also to the low microscopic uniformity of these alloys observed by SEM (Fig. 5).

The morphological and structural characteristics of the deposits obtained with the additive-free bath or using the A1 or A2 were very similar and, therefore, it is difficult to explain why A1 improves corrosion resistance. As mentioned above, these additives are usually included to reduce the stress in metallic deposition. Probably, the additive A1 promotes some changes in the first steps of the deposition process in such a way that the deposit is less stressed, but these changes cannot be observed in such thick deposits. The analysis of this process under controlled conditions may determine the role of these compounds in the deposition of zinc–nickel alloys.

The corrosion resistance of these alloys is also being measured by the usual a.c. and d.c. electrochemical techniques, in an attempt to relate the results with those obtained with the salt spray test.

4. Conclusions

Zinc–nickel alloys with satisfactory properties were obtained with a simple chloride bath containing NH_4Cl. At constant temperature, the composition and structure of the alloys obtained from an additive-free bath depended mainly on the bath composition and on the current density. Among the additives considered in the present study, only A3 promoted marked changes in the deposit characteristics: the nickel content was reduced, the dual-phase $\gamma + Zn$ was observed and the corrosion resistance was poor. However, there were no morphological or structural differences to explain the improvement of the corrosion behaviour observed when A1 was used. This process is now being analyzed under controlled conditions to determine the influence of the different parameters on the deposit characteristics, particularly the effect of the additive A1.

Acknowledgements

The authors are grateful to the DGICYT (Project number PB 90-0437) for financial assistance and to the Serveis Científico-Tècnics of the Universitat de Barcelona for the SEM, XRD and ESCA studies and absorption analysis. We thank Ministerio de Educación y Ciencia and CIRIT for financial support for G.B. and J.G.

References

[1] D. E. Hall, *Plat. Surf. Finish.* **70** (1983) 59.
[2] L. Felloni, R. Fratesi, E. Quadrini and G. Roventi, *J. Appl. Electrochem.* **17** (1987) 574.
[3] S. Sankarapapavinasam, F. Pushpanaden and M. F. Ahmed, *Metal Finish.* **85** (1987) 49.
[4] M. F. Mathias and T. W. Chapman. *J. Electrochem. Soc.* **134** (1987) 1408.
[5] G. Ramesh Bapu, G. Devaraj, J. Ayyapparaju and R. Subramanian, *Metal Finish.* **87** (1989) 9.
[6] C. H. Huang, *Plat. Surf. Finish.* **76** (1989) 64.
[7] R. Fratesi and G. Roventi, *J. Appl. Electrochem.* **22** (1992) 657.
[8] R. Albalat, E. Gómez, C. Müller, J. Pregonas, M. Sarret and E. Vallés, *ibid.* **20** (1990) 635.
[9] R. Albalat, E. Gómez, C. Müller, J. Pregonas, M. Sarret and E. Vallés, *ibid.* **21** (1991) 44.
[10] E. Gómez, C. Müller, M. Sarret, E. Vallés and J. Pregonas, *Metal Finish.* **90** (1992) 87.
[11] *US Patent 4 699 696* (1987).
[12] *US Patent 4 911 991* (1990).
[13] G. Z. Yin and D. W. Jillie, *Solid State Technol.* **30** (1987) 127.
[14] G. E. P. Box, W. G. Hunter and J. S. Hunter, 'Statistics for Experimentalists', John Wiley & Son, New York (1978).
[15] R. Fratesi and G. Roventi, Proceedings of Eurocorr, Vol I, Budapest, (21 October 1991) p. 165.
[16] M. Nikolova, I. Kristev, J. Cenov and L. Kristev, *B. Electrochem* **3** (1987) 649.
[17] J. Giridhar and W. J. Ooij, *Surf. Coat. Technol.* **52** (1992) 17.
[18] S. Swathirajan and Y. M. Mikhail, *J. Electrochem. Soc.* **136** (1989) 2188.